Regulation of SNARE complex assembly by an N-terminal domain of the t-SNARE Sso1p

Karin L. Nicholson[1], Mary Munson[2], Rebecca B. Miller[2,4], Thomas J. Filip[3],Robert Fairman[3] and Frederick M. Hughson[2]

The fusion of intracellular transport vesicles with their target membranes requires the assembly of SNARE proteins anchored in the apposed membranes. Here we use recombinant cytoplasmic domains of the yeast SNAREs involved in Golgi to plasma membrane trafficking to examine this assembly process *in vitro*. Binary complexes form between the target membrane SNAREs Sso1p and Sec9p; these binary complexes can subsequently bind to the vesicle SNARE Snc2p to form ternary complexes. Binary and ternary complex assembly are accompanied by large increases in α-helical structure, indicating that folding and complex formation are linked. Surprisingly, we find that binary complex formation is extremely slow, with a second-order rate constant of ~3 M^{-1} s^{-1}. An N-terminal regulatory domain of Sso1p accounts for slow assembly, since in its absence complexes assemble 2,000-fold more rapidly. Once binary complexes form, ternary complex formation is rapid and is not affected by the presence of the regulatory domain. Our results imply that proteins that accelerate SNARE assembly *in vivo* act by relieving inhibition by this regulatory domain.

SNARE proteins constitute core components of the machinery that docks and fuses intracellular transport vesicles in eukaryotes[1,2]. Significant evidence supports a model in which SNAREs anchored in the membrane of a transport vesicle (v-SNAREs) pair with SNAREs anchored in a target membrane (t-SNAREs) to form specific protein complexes that physically link the membranes[3,4]. Since distinct sets of SNAREs act in different intracellular transport steps, SNARE assembly provides a potentially general molecular mechanism for docking vesicles specifically at their correct intracellular destinations[5].

Recent evidence suggests that SNAREs also play a direct role in the subsequent fusion of vesicle and target membranes. Reconstituted into synthetic vesicles, SNAREs can mediate fusion, albeit slowly, demonstrating that they constitute a minimal fusion

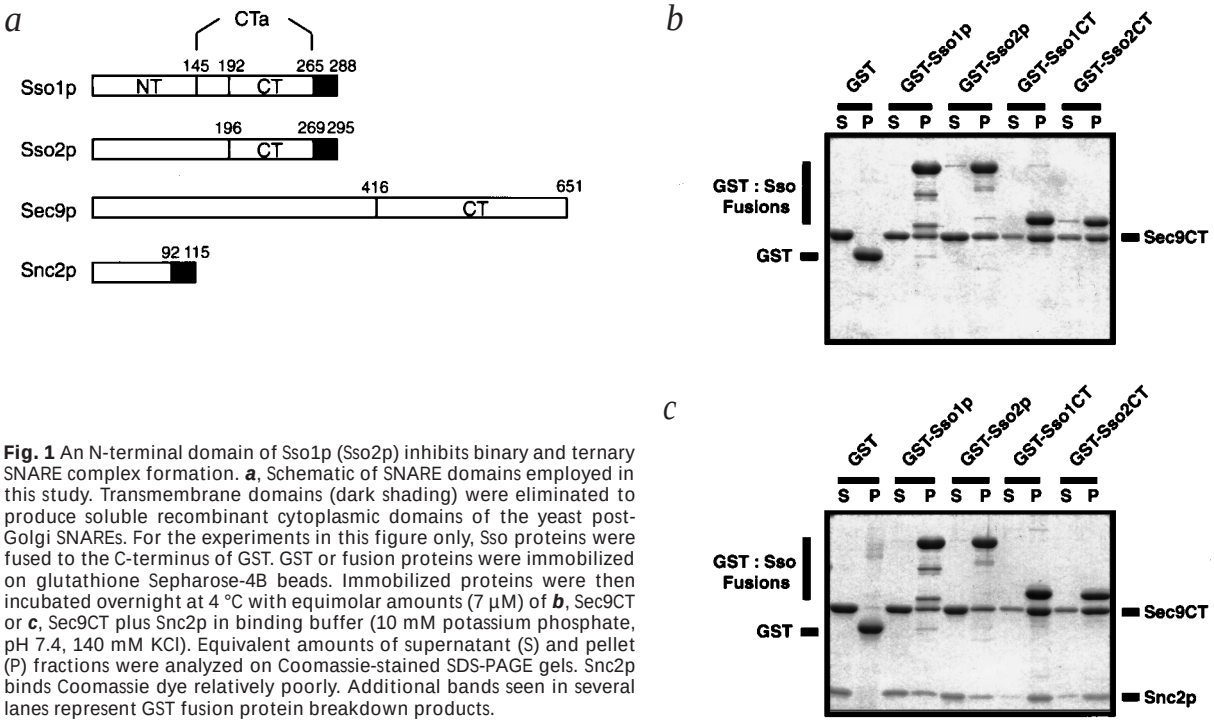

Fig. 1 An N-terminal domain of Sso1p (Sso2p) inhibits binary and ternary SNARE complex formation. ***a***, Schematic of SNARE domains employed in this study. Transmembrane domains (dark shading) were eliminated to produce soluble recombinant cytoplasmic domains of the yeast post-Golgi SNAREs. For the experiments in this figure only, Sso proteins were fused to the C-terminus of GST. GST or fusion proteins were immobilized on glutathione Sepharose-4B beads. Immobilized proteins were then incubated overnight at 4 °C with equimolar amounts (7 μM) of ***b***, Sec9CT or ***c***, Sec9CT plus Snc2p in binding buffer (10 mM potassium phosphate, pH 7.4, 140 mM KCl). Equivalent amounts of supernatant (S) and pellet (P) fractions were analyzed on Coomassie-stained SDS-PAGE gels. Snc2p binds Coomassie dye relatively poorly. Additional bands seen in several lanes represent GST fusion protein breakdown products.

[1]Department of Chemistry and [2]Department of Molecular Biology, Princeton University, Princeton, New Jersey 08544 and the [3]Department of Cell, Molecular, and Developmental Biology, Haverford College, Haverford, Pennsylvania 19041, USA. [4]Present address: Cellular Biochemistry and Biophysics Program, Memorial Sloan-Kettering Cancer Center, 1275 York Avenue, New York, New York 10021, USA.

Correspondence should be addressed to F.M.H. *email: fhughson@molbio.princeton.edu*

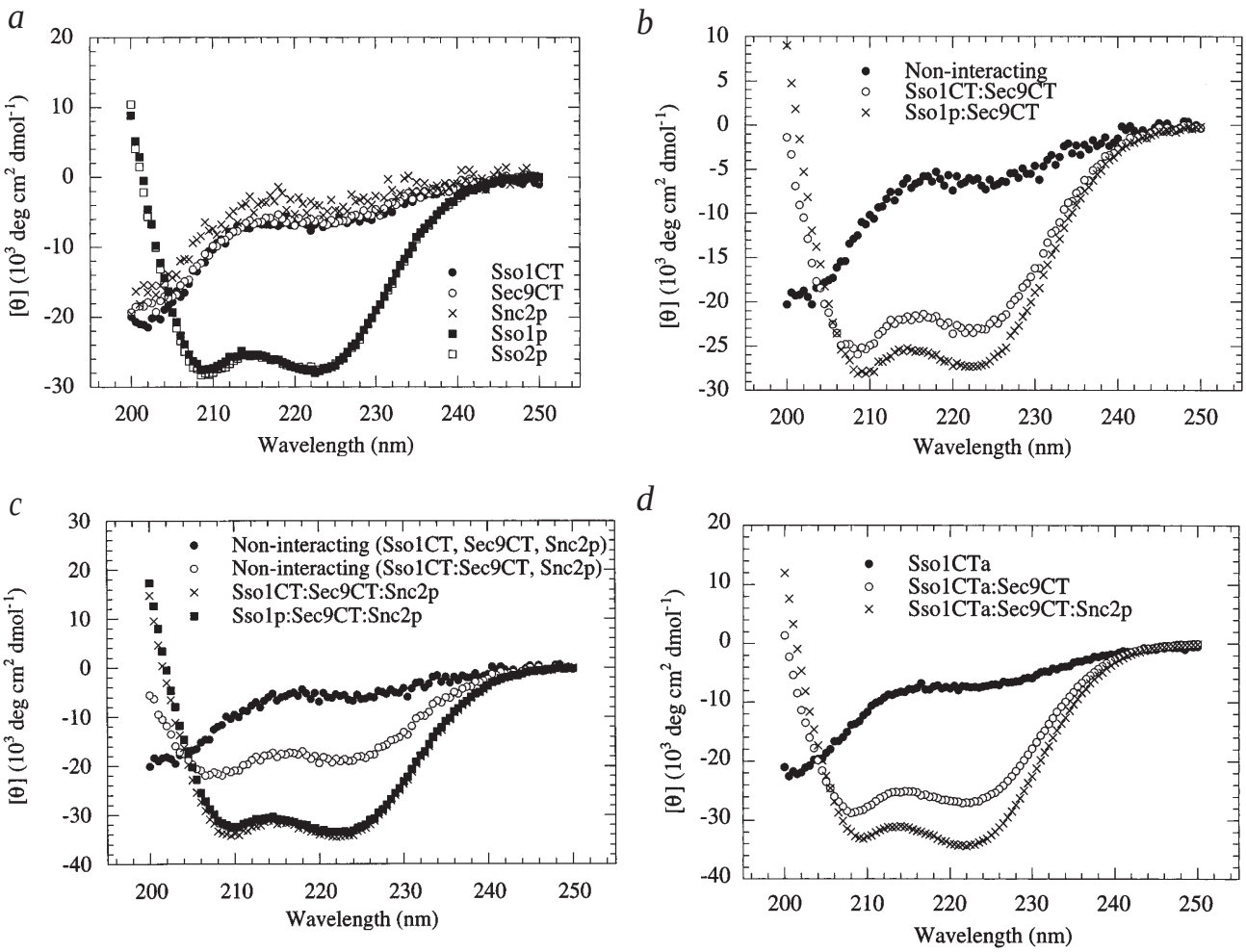

Fig. 2 Binary and ternary SNARE complex formation induces the folding of unstructured SNARE domains. CD spectra of the individual SNAREs and SNARE complexes (5 μM each) were acquired at 18 °C. ***a***, Spectra for Sso1CT, Sec9CT, Snc2p, Sso1p and Sso2p. ***b***, Sso1CT–Sec9CT displays substantially more helical structure (~60%) than predicted for a non-interacting mixture of Sso1CT and Sec9CT, but somewhat less than observed for Sso1p–Sec9CT. Note that [θ] is a per-residue value proportional to the fractional secondary structure content. Thus, the hypothetical 'non-interacting' spectrum is calculated as the residue-weighted mean of the Sso1CT and Sec9CT spectra shown in (*a*). ***c***, Ternary SNARE complexes Sso1CT–Sec9CT–Snc2p and Sso1p–Sec9CT–Snc2p are both >85% α-helical. For comparison, the predicted spectra for a non-interacting mixture of the individual SNAREs Sso1CT + Sec9CT + Snc2p and Sso1CT–Sec9CT + Snc2p are shown. ***d***, Spectra for Sso1CTa, Sso1CTa–Sec9CT and Sso1CTa–Sec9CT–Snc2p.

machinery[6]. Low-resolution structural studies of neuronal SNARE complexes show that the transmembrane anchors of the participating v- and t-SNAREs are at the same end of an elongated complex[7,8]. This geometry, which bears some similarity to that of the fusion proteins of enveloped viruses including influenza and HIV-1[9], may promote close membrane apposition, leading to fusion[6–8].

Golgi to plasma membrane transport in yeast involves at least one v-SNARE, Snc1p (or the functionally redundant Snc2p), and two t-SNAREs, Sec9p and Sso1p (or the functionally redundant Sso2p)[10–12]. These yeast SNAREs show significant sequence homology to neuronal SNAREs (VAMP/synaptobrevin, SNAP-25 and syntaxin respectively) required for the fusion of synaptic vesicles with the presynaptic membrane[13,14]. Snc1p (Snc2p) is localized predominantly to post-Golgi vesicles[10], whereas Sso1p (Sso2p) is localized predominantly to the plasma membrane[11,12]; both are type II integral membrane proteins with C-terminal transmembrane anchors. To form v-SNARE–t-SNARE complexes, Snc and Sso proteins appear to require the collaboration of a second plasma-membrane-localized t-SNARE, Sec9p[15]. Unlike most SNAREs, Sec9p is a peripheral membrane protein that lacks a plausible transmembrane anchor[11]. Its neuronal homolog SNAP-25 is multiply palmitoylated[16], but Sec9p, which lacks cysteine residues, is not. The basis for Sec9p's plasma membrane localization is not known. Despite forming stable binary complexes with Sso proteins *in vitro*, Sec9p's association with the plasma membrane appears to be independent of Sso proteins *in vivo* (ref. 15 and P. Brennwald, pers. comm.). It may instead interact directly with phospholipids or with an unidentified plasma membrane receptor.

These yeast SNAREs, like their neuronal counterparts, form complexes *in vivo* and *in vitro*[3,11,17,18]. Individual SNAREs frequently contain one or more 4,3 hydrophobic (heptad) repeat regions potentially capable of forming α-helical coiled coils[18–23]. The rough coincidence between these regions and the minimal fragments required for binding other SNAREs *in vitro* suggests that SNARE complex formation may occur through the formation of coiled coils[18,21,22]. Consistent with this possibility, recombinant cytoplasmic SNARE domains can be assembled *in vitro* to form stable bina-

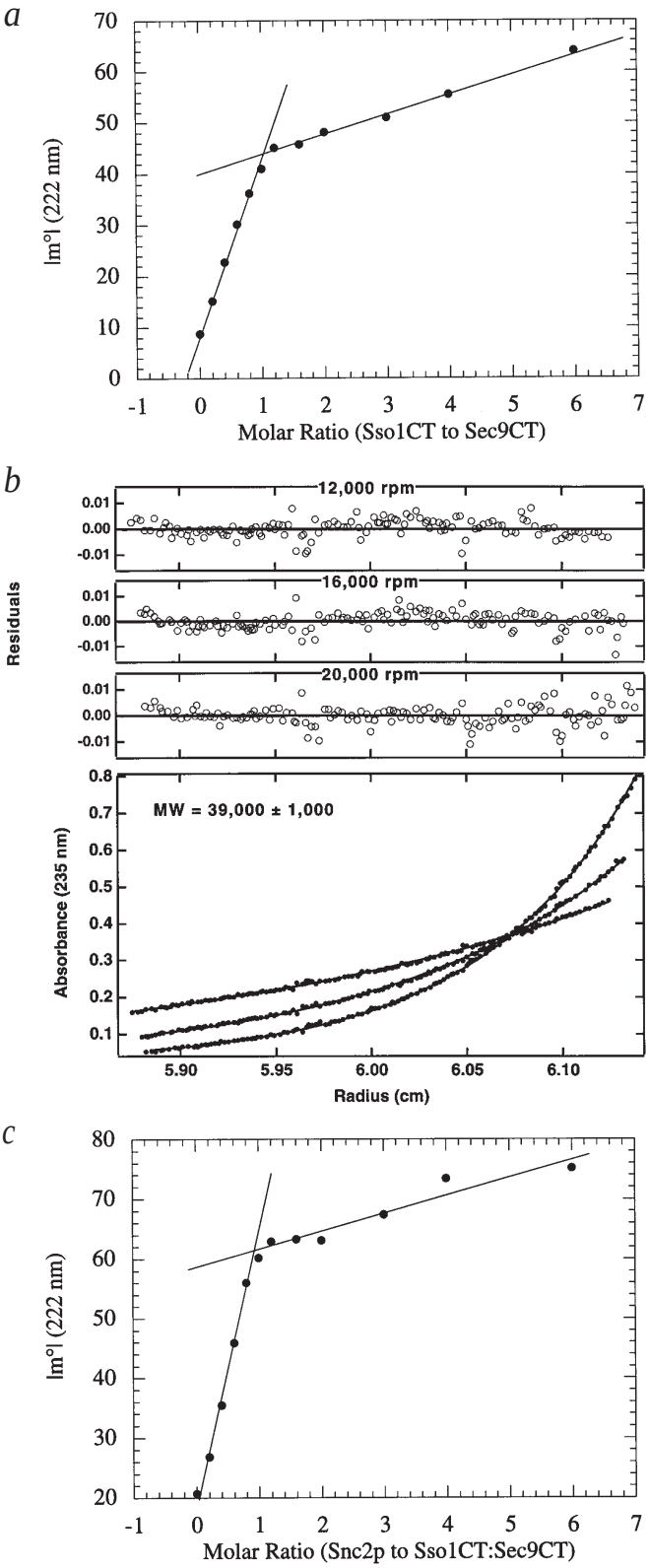

Fig. 3 Binary and ternary SNARE complex stoichiometries. ***a***, The CD signal at 222 nm (4 °C) for 5 μM Sec9CT plus varying concentrations (0–30 μM) of Sso1CT. The absolute value of the raw signal, |m°|, is shown, uncorrected for concentration. ***b***, Sedimentation equilibrium analysis of a 1:1 mixture of Sso1CT and Sec9CT (5 μM each) at 4 °C. Data from the three rotor speeds shown were fit simultaneously to a single-species model, yielding a relative molecular mass of 39,000 ± 1,000 M_r, in reasonable agreement with the predicted molecular mass of 36,095. Residuals from the curve fits are also shown. Low temperature was used in (*a*) and (*b*) because the Sso1CT–Sec9CT complex is partially dissociated at 18 °C (see Fig. 4*a*). ***c***, The CD signal at 222 nm (18 °C) for 0.5 μM Sso1CT–Sec9CT plus varying concentrations (0–3 μM) of Snc2p.

ry (Sso1p–Sec9p or syntaxin–SNAP-25) and ternary complexes in reactions accompanied by substantial increases in α-helicity[15,18,24–26].

SNARE complex assembly and disassembly appears to be regulated by other proteins known to be essential for the proper functioning of the secretory pathway[27]. Small GTP-binding Rab proteins are essential for SNARE assembly *in vivo*[28–30], whereas Sec1p family members bind t-SNAREs and can inhibit SNARE complex formation *in vitro*[30–32]. Members of the NSF/p97 family, in conjunction with accessory proteins, can function as molecular chaperones by disassembling SNARE complexes in an ATP-dependent reaction[3].

Here, we take advantage of the favorable solution properties displayed by cytoplasmic domains of the yeast post-Golgi SNAREs to carry out quantitative *in vitro* studies of SNARE assembly. We demonstrate that complex formation by the full-length cytoplasmic domain of Sso1p is exceedingly slow, although given sufficient time it does proceed to completion. Truncated versions of Sso1p lacking an N-terminal domain form complexes much more rapidly. SNARE complexes containing truncated Sso1p are essentially identical in terms of structure and stability to those containing the intact cytoplasmic domain of Sso1p. Therefore, binary and ternary SNARE complex formation is kinetically controlled by the N-terminal regulatory domain of the t-SNARE Sso1p. These results suggest a plausible mechanism for factors that control SNARE assembly *in vivo*.

N-terminal Sso1p domain inhibits complex formation

Binary t-SNARE complex formation was observed when GST fusion proteins containing the cytoplasmic regions of Sso1p or Sso2p were incubated with a C-terminal domain of Sec9p (Fig. 1*a*,*b*). This Sec9p domain (Sec9CT; residues 416–651) is the sole essential region of Sec9p *in vivo*[11] and the only region with detectable sequence homology to the neuronal t-SNARE SNAP-25. For these reasons, and because full-length recombinant Sec9p is poorly soluble, all experiments reported here were carried out with Sec9CT. In agreement with previous studies[15], GST-Sso1p bound a substantial, though substoichiometric, amount of Sec9CT after overnight incubation at 4 °C. GST-Sso2p gave very similar results, as expected based on the functional redundancy and 72% amino acid identity between Sso1p and Sso2p. Ternary complexes form upon addition of the cytoplasmic domain of the post-Golgi v-SNARE Snc2p (Fig. 1*c*), as has been seen for the functionally redundant (and 83% identical) Snc1p[15]. These results suggest that, regardless of the Snc or Sso isoform used, binary and ternary complex assembly occurs, but is inefficient.

By contrast, a 74-residue C-terminal region of either Sso protein forms binary and ternary complexes much more efficiently under the same conditions (Fig. 1). These constructs, GST-Sso1CT and GST-Sso2CT, comprise the region homologous to the minimal SNARE-binding domain of syntaxin[18,21]. The discrepancy between full-length and C-terminal Sso constructs is consistent with previous results[15] and suggests that an N-terminal regulatory domain in each Sso protein inhibits SNARE complex formation. This regulation could be thermodynamic or kinetic in

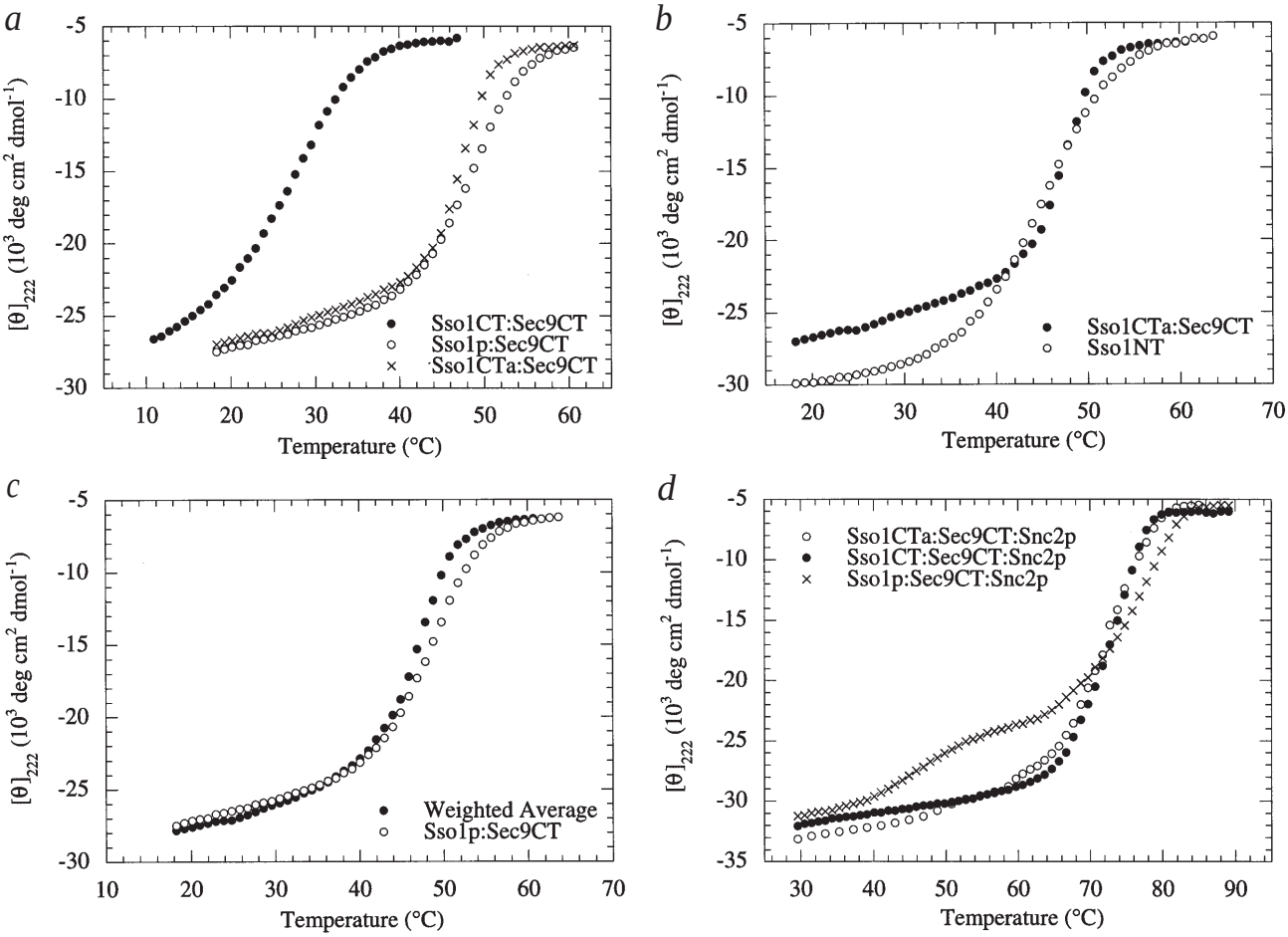

Fig. 4 The high thermal stability of binary and ternary SNARE complexes is independent of the Sso1p N-terminal domain. The thermal stabilities of binary (*a*–*c*) and ternary (*d*), SNARE complexes (5 μM each in binding buffer) were evaluated by monitoring [θ] at 222 nm as a function of temperature. ***a***, Thermal denaturation of Sso1CT–Sec9CT (T_m = 26 °C), Sso1CTa–Sec9CT (T_m = 47 °C), and Sso1p–Sec9CT (T_m = 48 °C). ***b***, Thermal denaturation of Sso1NT (T_m = 45 °C) and Sso1CTa–Sec9CT (T_m = 47 °C). ***c***, The observed thermal denaturation profile for the Sso1p–Sec9CT binary complex is similar to that predicted for the residue-weighted average of the profiles shown in (*b*). ***d***, Thermal denaturation of Sso1CT–Sec9CT–Snc2p (T_m = 72 °C), Sso1CTa–Sec9CT–Snc2p (T_m = 73 °C), and Sso1p–Sec9CT–Snc2p. The irreversible unfolding of Sso1p–Sec9CT–Snc2p entails at least two transitions: the first (T_m = 45 °C) corresponds to unfolding of the Sso1NT domain, while the second (T_m ~75–80 °C) may represent unfolding of the coiled coil core (see text).

origin. In one case, Sso1CT–Sec9CT complexes could be more stable (lower K_D) than Sso1p–Sec9CT complexes[15]. Alternatively, binary (and hence ternary) complex formation could be unusually slow in the presence of the N-terminal regulatory domain of Sso1p (Sso2p), so that complex formation is incomplete even after overnight incubation. Surprisingly, the latter proves to be the case.

Assembly-induced folding of SNARE domains

To establish that Sso1CT and Sso1p form SNARE complexes with similar properties, we compared the secondary structural content, stoichiometry and stability of these complexes. Initially, we measured the secondary structure contents of the individual SNARE domains using circular dichroism (CD). Sec9CT is largely lacking in regular secondary structure (Fig. 2*a*), as was also observed for a similar C-terminal fragment of Sec9p[26] and for several neuronal SNAP-25 isoforms[24,25]. Likewise, Snc2p appears to be unfolded as judged by CD spectroscopy (Fig. 2*a*) and amide proton exchange experiments (data not shown), in accord with previous reports for Snc2p homologs[26,33]. Unlike Sso1p and Sso2p, which display CD spectra indicative of substantial (~70%; see Methods) α-helix content, Sso1CT and Sso2CT are largely unfolded (Fig. 2*a*). Therefore, the SNARE regions that form binary and ternary complexes efficiently all seem, individually, to lack significant regular secondary structure.

A dramatic acquisition of α-helical secondary structure accompanied the combination of Sso1CT and Sec9CT in a 1:1 molar ratio, with the final α-helix content of ~60% (Fig. 2*b*). The observed spectrum for Sso1CT–Sec9CT differs significantly from that anticipated for a non-interacting mixture, indicating that binary complex formation is coupled to significant folding of one or both of the largely-unstructured t-SNARE domains. The chromatographically-purified Sso1p–Sec9CT complex, with the full-length cytoplasmic domain of Sso1p, displays an α-helix content of ~70% (Fig. 2*b*). These results demonstrate that, in terms of secondary structure, the Sso1CT–Sec9CT and Sso1p–Sec9CT complexes are similar; indeed, the small discrepancy arises predominantly from the marginal stability of Sso1CT–Sec9CT.

The sharp increase in helix content observed upon Sso1CT–Sec9CT complex formation was used to establish the saturability and molar ratio of the binding reaction. When Sso1CT was titrated into a constant amount of Sec9CT (Fig. 3*a*), a break in the plot of ellipticity versus concentration was seen at a 1:1 molar

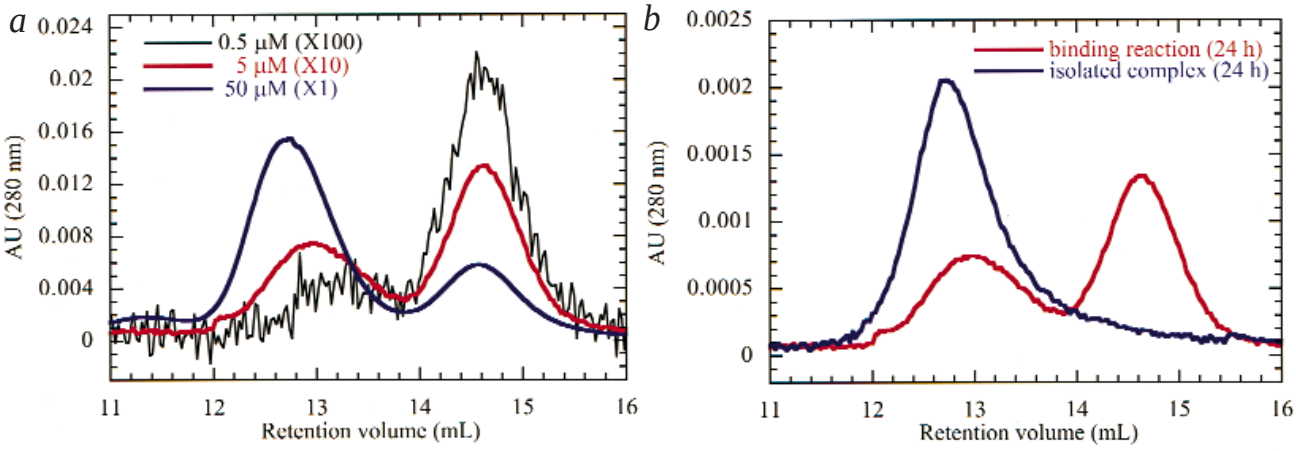

Fig. 5 Binary Sso1p–Sec9CT complex assembly approaches equilibrium slowly. ***a***, Equimolar mixtures of Sso1p and Sec9CT in binding buffer were incubated 24 h at 4 °C before separation on a Superdex 200 gel filtration column (Pharmacia) equilibrated in the same buffer. Overlaid profiles are shown for 0.5 μM, 5 μM, and 50 μM each (Sso1p and Sec9CT). To facilitate comparison, the absorbance for the 0.5 and 5 μM samples were scaled appropriately as shown. In control experiments (not shown), Sso1p–Sec9CT elutes at 12.7 ml, Sec9CT elutes at 13.3 ml, and Sso1p elutes at 14.6 ml. In addition, gel filtration of Sso1p alone at concentrations above 100 μM showed no evidence of self-association. The molar extinction coefficient of Sso1p is about four times greater than that of Sec9CT. The Sec9CT peak overlaps with the binary complex peak and can cause apparent shifts in its elution volume when the ratio of free Sec9CT to binary complex is high. ***b***, Isolated Sso1p–Sec9CT complex (5 μM) was incubated 24 hr at 4 °C and analyzed as in (*a*). 5 μM Sso1p and 5 μM Sec9CT, mixed and subjected to the same incubation, are only partially complexed after 24 h.

ratio, with a further slow increase in signal attributable to the small contribution of uncomplexed (and hence unfolded) Sso1CT. Equilibrium sedimentation analytical ultracentrifugation (Fig. 3*b*) showed that the complex contains one molecule each of Sso1CT and Sec9CT. As expected[26], Sso1p–Sec9CT complexes are also 1:1 (MW=59,500 ± 2,200; data not shown). Therefore, the oligomeric state of the yeast binary complex is unchanged by deletion of the N-terminal domain of Sso1p.

The addition of Snc2p to Sso1CT–Sec9CT binary complexes resulted in a further large increase in α-helix content, to a total value of greater than 85% (Fig. 2*c*). The high helix content of the ternary complex suggests strongly that Snc2p folds to adopt an α-helical structure upon binding to the binary t-SNARE complex and that one or both t-SNAREs also adopt additional helical structure. Comparing the CD spectra of ternary complexes assembled from Sso1CT and Sso1p (Fig. 2*c*) reveals that these complexes have very similar secondary structural contents.

Ternary Sso1CT–Sec9CT–Snc2p complex formation is saturable at a 1:1:1 molar ratio (Fig. 3*c*). However, the results of analytical ultracentrifugation experiments were not consistent with a single species, but instead revealed that higher-order structures coexist in equilibrium with 1:1:1 complexes even at low (1–5 μM) protein concentrations (data not shown). Although the significance of these higher-order structures is not clear, ternary complexes containing the full-length cytoplasmic domain of Sso1p behave similarly[26]. Therefore, the absence of the N-terminal Sso1p domain has little or no impact, either in terms of secondary structure or oligomeric state, on the properties of binary and ternary complexes.

Complex stability is unaffected by Sso1NYT domain

The stability of each SNARE complex was evaluated by monitoring the CD signal at 222 nm as a function of temperature. Except for Sso1p–Sec9CT and Sso1p–Sec9CT–Snc2p complexes, which refold slowly, thermal denaturation was fully reversible. The stability of the Sso1CT–Sec9CT complex was marginal (Fig. 4*a*); indeed, Sso1CT–Sec9CT complexes were significantly less stable than Sso1p–Sec9CT complexes. This explains the origin of the difference in helix content between these complexes when measured at 18 °C (Fig. 2*b*). To determine whether Sso1CT was lacking residues required to confer full stability on the binary complex, we tested a longer construct (Sso1CTa) containing residues 146–265 (Fig. 1*a*). This fragment represents the entire cytoplasmic domain of Sso1p except for the N-terminal domain defined by limited proteolysis (Sso1NT; residues 1–145; M.M. & F.M.H., unpublished results). In most respects, Sso1CTa and Sso1CT displayed identical properties (Fig. 2*d* and data not shown) with one major exception: Sso1CTa–Sec9CT complexes are nearly as stable as Sso1p–Sec9CT complexes (Fig. 4*a*). Therefore, the 'minimal SNARE-binding domain' (Sso1p 192–265) is missing sequences that participate in stabilizing the binary complex. However, the presence or absence of the Sso1NT domain has little effect.

The unfolding curve for Sso1p–Sec9CT may in fact represent the sum of two independent contributions: the unfolding of the Sso1NT domain, and the unfolding of the rest of the complex. Consistent with this hypothesis, the thermal unfolding curve for Sso1p–Sec9CT is similar to the residue-weighted average of the curves for Sso1NT and Sso1CTa–Sec9CT, measured separately (Fig. 4*b*,*c*). The small residual difference suggests that Sso1p–Sec9CT may be modestly stabilized by the presence of the N-terminal domain. The low-temperature baselines in Fig. 4*c* coincide, providing quantitative evidence for the similarity in secondary structures between complexes including or lacking the Sso1NT domain (compare Fig. 2*b*).

The addition of Snc2p to the binary complexes yields very stable ternary complexes (Fig. 4*d*). The thermal denaturation profile of Sso1p–Sec9CT–Snc2p displays at least two transitions. The first transition, centered around 45 °C, is quantitatively consistent with independent unfolding of the Sso1NT domain (Fig. 4*b*). Electron micrographs show that an N-terminal domain of syntaxin projects from one end of the rod-like core of the neuronal ternary SNARE complex[7]. Our results provide thermodynamic evidence that, in the corresponding yeast complex, this domain is independent.

At temperatures around 75–80 °C, the remainder of the α-helical structure (~350 helical residues) unfolds somewhat cooperatively.

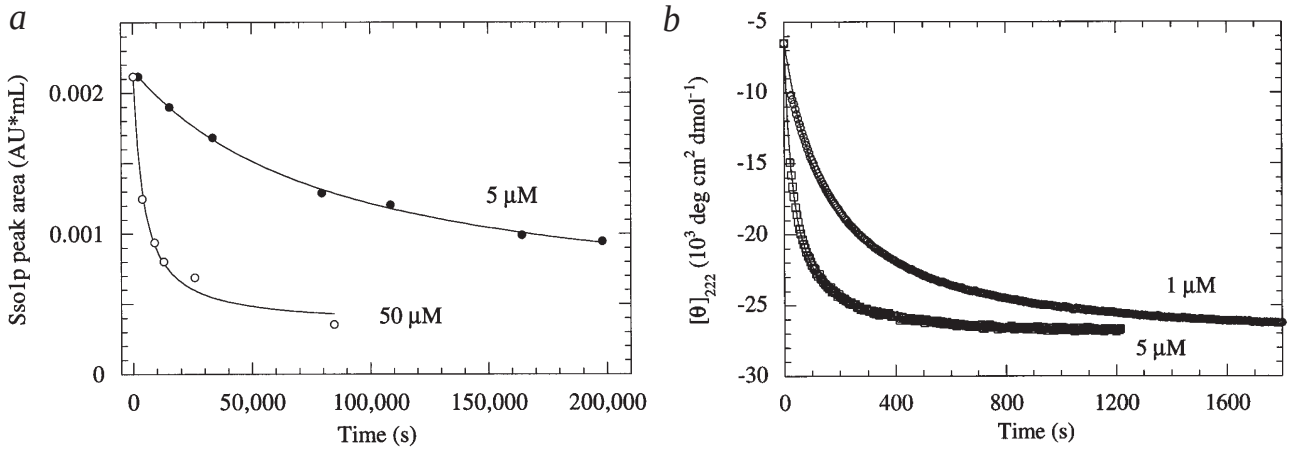

Fig. 6 Formation of Sso1p–Sec9CT binary complex is inhibited by the N-terminal domain of Sso1p. ***a***, Equimolar mixtures of Sso1p and Sec9CT in binding buffer were incubated at 18 °C, during which aliquots were removed and analyzed by gel filtration as in Fig. 5. Binary complex formation was monitored as the disappearance of the Sso1p peak over time. Data for typical experiments at 5 μM (200 μl injections) and 50 μM (20 μl injections) protein concentrations are shown fit to a second order rate equation as described in the Methods. For two separate experiments at 5 μM, the rate constant (k) obtained was 2.2 ± 0.2 M^{-1} s^{-1}. Similarly, for two experiments at 50 μM, a rate constant of 3.1 ± 2.5 M^{-1} s^{-1} was obtained. ***b***, Equimolar Sso1CTa and Sec9CT in binding buffer were mixed and monitored over time by CD at 222 nm, 18 °C. Data were well-fit by the bimolecular second order rate equation used in (*a*); however, the derived rate constants for 1 μM (k = 7100 ± 200 M^{-1} s^{-1}) and 5 μM (k = 6300 ± 200 M^{-1} s^{-1}) reactant concentrations are ~2,000-fold faster than seen for Sso1p–Sec9CT complex formation. For each experiment, the mean and standard deviation are given for two separate experiments. ***c***, Sso1NT binds to Sso1CT. Sso1NT (30 μM) and Sso1CT (0, 30, 60 or 120 μM) in binding buffer were mixed and incubated 10' on ice prior to gel filtration analysis. Only Sso1NT contributes to the absorbance profile, as Sso1CT lacks Tyr, Trp, and Cys residues. No absorbance is detected outside the displayed volume range.

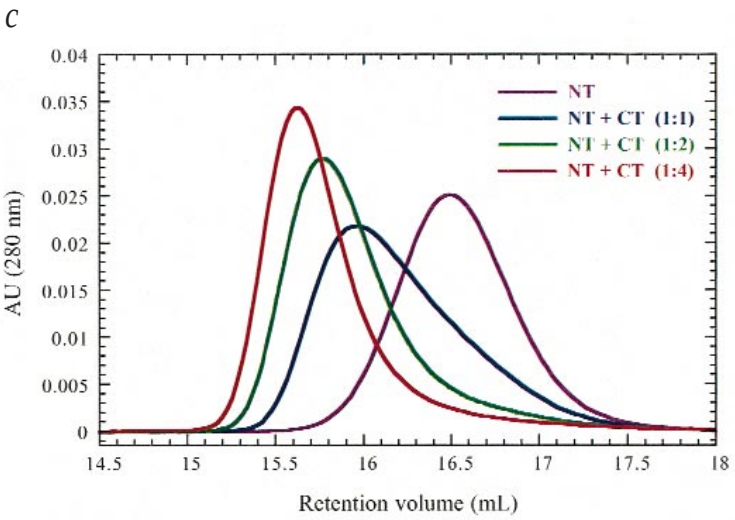

Assuming that the structure of the ternary yeast complex resembles that seen for the neuronal complex[7], this transition likely corresponds to unfolding of the rod-like core. Both truncated complexes (Sso1CT–Sec9CT–Snc2p and Sso1CTa–Sec9CT–Snc2p), which lack the Sso1NT domain, unfold in single cooperative transitions. Our ability to compare the stabilities of truncated and full-length complexes is compromised by the incomplete cooperativity and effective irreversibility of the Sso1p–Sec9CT–Snc2p unfolding transition(s). Nonetheless, taken together, our results demonstrate that the overall structure and stability of SNARE complexes are essentially unaffected by deletion of the Sso1NT domain.

Binary t-SNARE complexes assemble slowly

To characterize the process of binary and ternary complex assembly, we developed binding assays that circumvent the need for fusion proteins or immobilization of one of the binding partners. In an initial experiment, we mixed equimolar amounts of Sso1p and Sec9CT, incubated for 24 h at 4 °C, and then separated uncomplexed from complexed Sso1p using gel filtration (Fig. 5*a*). Complex formation is monitored as an increase in the area of the Sso1p–Sec9CT peak and a concomitant decrease in the area of the free Sso1p peak. The apparent position of the Sso1p–Sec9CT complex is displaced slightly by the presence of free Sec9CT, which otherwise has little effect on the chromatogram because of its low extinction coefficient (Fig. 5 legend). In agreement with GST fusion protein binding studies, we found that Sso1p–Sec9CT complex assembly was inefficient, although at the highest concentrations >80% complex formation could be observed.

Surprisingly, binding reactions at these concentrations were not at equilibrium after 24 h. For example, we found that 5 μM purified Sso1p–Sec9CT complex, incubated 24 h at 4 °C, does not dissociate detectably into monomers, whereas 5 μM Sso1p mixed with 5 μM Sec9CT, after the same incubation, yields only ~30% complex (Fig. 5*b*). This discrepancy between two samples of identical composition suggests that association:dissociation is remarkably slow. The alternative possibility that a significant fraction of the monomers are incompetent for complex formation can be ruled out because complex formation is nearly quantitative at high monomer concentrations (Fig. 5*a*). Other potential complications are ruled out by analytical ultracentrifugation studies showing that Sso1p, Sec9CT, and the binary complex are all monomeric (or 1:1) under these conditions (data not shown).

To characterize what thus appears to be very slow association, we followed the progress of complex assembly using this gel filtration assay (Fig. 6*a*). The data at two different protein concentrations (5 and 50 μM of each protein) are consistent with a simple second-order bimolecular binding reaction (Sso1p + Sec9CT → Sso1p–Sec9CT). The resulting second order rate constant of 2–3 M^{-1} s^{-1} is, however, unusually slow: at 5 μM concentrations of each protein, the half-time of the binding reaction is ~20 h, and

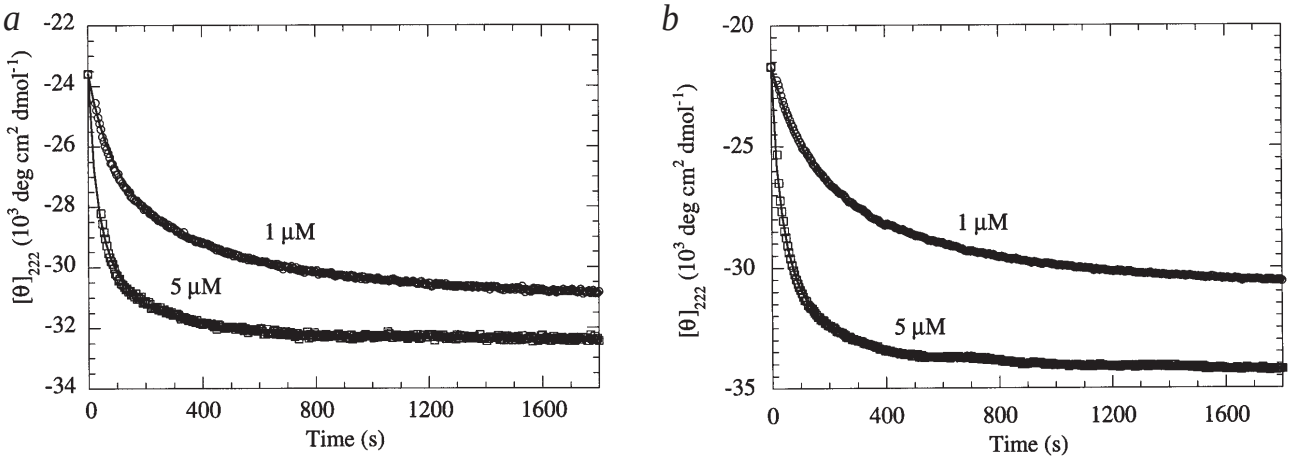

Fig. 7 Formation of the binary complex is rate-limiting for ternary complex assembly. Equimolar mixtures of pre-formed ***a***, Sso1p–Sec9CT or ***b***, Sso1CTa–Sec9CT were mixed manually with Snc2p and monitored over time by CD at 222 nm, 18 °C for 1 μM and 5 μM final concentrations of each protein. Again, these data fitted well to the bimolecular rate equation (see Methods), consistent with the reaction SsoX–Sec9CT + Snc2p → SsoX–Sec9CT–Snc2p (where SsoX is Sso1CTa or Sso1p). For all reactions, the derived rate constant was very similar: for Sso1CTa at 1 μM, k = 5,800 ± 1,100 M^{-1} s^{-1}; for Sso1CTa at 5 μM, k = 5,000 ± 300 M^{-1} s^{-1}; for Sso1p at 1 μM, k = 5,800 ± 2,000 M^{-1} s^{-1}; and for Sso1p at 5 μM, k = 6,100 ± 1,200 M^{-1} s^{-1}. For each, the mean and standard deviation are given for two separate experiments.

very high effective concentrations (>1 mM) would be required to achieve assembly on a plausible time scale *in vivo*. These results are biologically intriguing, since they imply that other factors must play critical roles in accelerating association.

Removal of Sso1NT domain accelerates assembly

Because the rate of binary complex formation by Sso1p is orders of magnitude slower than expected for physiological systems, it seemed plausible that the intact protein contains a regulatory domain that inhibits complex assembly. An attractive candidate, based on GST pulldown experiments (Fig. 1), was the N-terminal domain of Sso1p. To test this hypothesis, we monitored complex formation between soluble Sso1CTa and Sec9CT. Complex formation was already complete at the earliest time points and lowest protein concentrations achievable in the gel filtration assay (data not shown). As an alternative, therefore, we used the structural changes that accompany binary complex formation to monitor this assembly process using CD at 222 nm (Fig. 6*b*). Again, a simple second-order rate law fits the data at two different protein concentrations. Strikingly, we found that the rate constant for Sso1CTa–Sec9CT complex assembly (6–7 × 10^3 M^{-1} s^{-1}) is more than three orders of magnitude faster than that for Sso1p–Sec9CT assembly. The shorter Sso1CT construct formed binary complexes with essentially identical kinetics (5.8 ± 0.8 × 10^3 M^{-1} s^{-1}; data not shown). We also reexamined Sso1p–Sec9CT assembly using this CD assay with results (k = 3.9 ± 1.1 M^{-1} s^{-1} for experiments with 20 μM each protein) very similar to those obtained by gel filtration. Thus, deleting the Sso1NT domain accelerates binary complex formation ~2,000-fold, implicating this domain in the regulation of SNARE complex assembly.

Even the relatively fast association and folding of Sso1CTa–Sec9CT is ~100-fold slower than that observed for previously-studied homodimeric coiled coils[34]. Nonetheless, under the conditions employed in this study, folding shows two-state behavior: the entire magnitude of the CD signal change during the folding process is accounted for by a single kinetic phase, with no evidence for faster-folding phases during the dead-time of manual mixing.

We postulated that the Sso1NT domain may block binary complex formation by interacting intramolecularly with the Sso1CT domain. Consistent with this hypothesis, we find that the separate Sso1NT and Sso1CT domains bind one another (Fig. 6*c*). Binding is observed as a shift in the gel filtration elution volume of Sso1NT caused by binding to Sso1CT, which does not itself absorb at 280 nm. Tailing of the complex peak establishes that the off-rate is significant relative to the time required for gel filtration (~20 min). Although these experiments suggest that Sso1NT–Sso1CT binding in *trans* is relatively weak, the effective concentration of the two domains within the intact protein may be very high. Sso1NT–Sso1CT binding is not accompanied by a detectable net change in secondary structure (data not shown).

Rapid ternary complex formation

Ternary complexes assemble rapidly upon mixing Snc2p with pre-formed Sso1p–Sec9CT or Sso1CTa–Sec9CT (Fig. 7). Like binary complex formation, ternary complex formation is well-described by a second-order reaction (Sso–Sec9CT + Snc2p → Sso–Sec9CT–Snc2p). The rate constant (~6 x 10^3 M^{-1} s^{-1}; see Fig. 7 legend) is not affected by the presence or absence of the Sso1NT domain. For Sso1CTa–Sec9CT–Snc2p, the final α-helicity is somewhat concentration-dependent (Fig. 7*b*), possibly because the formation of higher-order structures is accompanied by further α-helix formation.

These results, together with our inability to observe Sec9CT–Snc2p or Sso–Snc2p complexes even at high (>10 μM) protein concentrations (data not shown), argue strongly that yeast post-Golgi SNARE complex formation *in vitro* occurs through a rate-limiting Sso1p–Sec9CT assembly step, after which ternary complex formation is relatively rapid (Fig. 7). Furthermore, they establish that the Sso1NT regulatory domain inhibits only binary complex formation, not ternary complex formation.

Functional implications

The recent finding that v–t SNARE complexes are sufficient to mediate membrane fusion[6] suggests that regulating their assembly is crucial in controlling the activity and specificity of the cellular membrane fusion machinery. Our results show that an N-terminal domain of Sso1p (Sso1NT) is a potent intramolecular inhibitor of binary SNARE complex formation. The Sso1NT domain inhibits

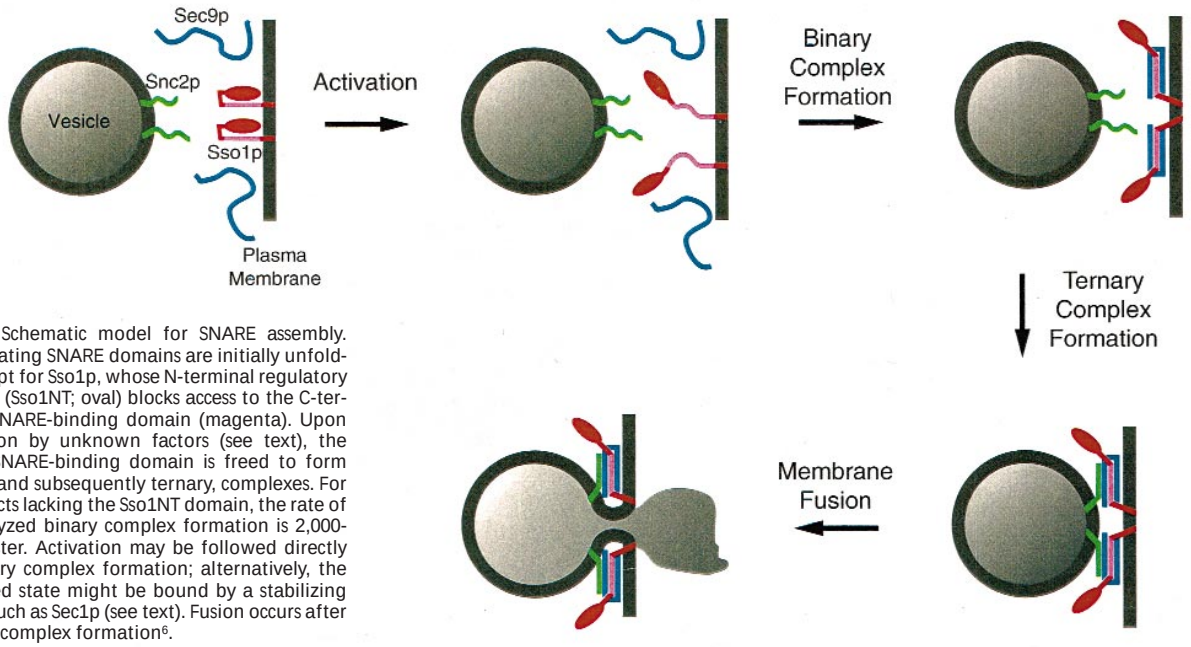

Fig. 8 Schematic model for SNARE assembly. Participating SNARE domains are initially unfolded except for Sso1p, whose N-terminal regulatory domain (Sso1NT; oval) blocks access to the C-terminal SNARE-binding domain (magenta). Upon activation by unknown factors (see text), the Sso1p SNARE-binding domain is freed to form binary, and subsequently ternary, complexes. For constructs lacking the Sso1NT domain, the rate of uncatalyzed binary complex formation is 2,000-fold faster. Activation may be followed directly by binary complex formation; alternatively, the activated state might be bound by a stabilizing factor such as Sec1p (see text). Fusion occurs after ternary complex formation[6].

complex formation by a kinetic mechanism, slowing the rate of this assembly reaction 2,000-fold (Fig. 6*a*,*b*). The stability of the complex, once formed, is relatively insensitive to the presence of the Sso1NT domain (Fig. 4), ruling out an alternative, primarily thermodynamic, model. Binary t-SNARE complex formation is likely to be rate-limiting for the overall SNARE assembly reaction, since preformed binary complexes form ternary complexes rapidly (Fig. 7).

The Sso1NT domain appears to block complex formation by interacting intramolecularly with the C-terminal SNARE-binding domain (Fig. 8). The isolated Sso1NT domain binds Sso1CT (Fig. 6*c*), albeit with modest affinity. In intact Sso1p, it is entirely plausible that the effective concentration of the covalently-attached Sso1NT domain is sufficiently high to slow binary SNARE complex formation dramatically. In this case, SNARE complex formation in the absence of additional activating factors would need to await the infrequent spontaneous release of the C-terminal domain.

Although Sso1p and Sec9p are both localized to the plasma membrane *in vivo*, only a very small fraction of the Sec9p (<1%) is associated with Sso1p in extracts (P. Brennwald, pers. comm.). We find that binary complexes are stable, arguing against the possibility that they fall apart during isolation. Thus, only a small pool of assembled (that is, active) binary t-SNARE complex appears to exist at steady state *in vivo*. Since we have found that the rate of spontaneous Sso1p–Sec9p assembly is unphysiologically slow, we propose that assembly is catalyzed *in vivo* by factors that regulate docking and/or fusion (Fig. 8).

Although Sso1p and Sec9p are found throughout the periphery of the cell, assembly of binary complexes could be restricted by localized activating factors. Such activating factors could serve to spatially restrict Sso1p–Sec9p activity to the bud tip, the site of exocytosis in yeast[35]. In principal, any specialized feature of the bud tip could serve to release Sso1NT inhibition. Several proteins or protein complexes, including the so-called Exocyst complex[36,37], are found specifically at the bud tip and, as such, are particularly attractive candidates.

Post-Golgi vesicles may also carry factors that can activate binary t-SNARE complex assembly in response to vesicle arrival. Members of the Rab family of small Ras-like GTPases, localized on vesicles, have been shown to facilitate vesicle docking and/or SNARE assembly[28–30,38]. For trafficking from the Golgi to the plasma membrane in yeast, genetic evidence places the relevant Rab protein (Sec4p) upstream of Sec9p[11]. Our results suggest that upstream activators including Sec4p may influence Sec9p activity through Sso1p, by relieving the intramolecular inhibition exerted by the Sso1NT domain.

Members of the Sec1 protein family can also influence SNARE assembly through interactions with t-SNAREs. In fact, *SSO1* and *SSO2* were originally isolated as high copy suppressors of temperature-sensitive *sec1* mutants[12]. Although evidence for a direct physical interaction between Sso1p (Sso2p) and Sec1p has not been reported, their neuronal counterparts syntaxin and the peripheral membrane protein n-Sec1 form tight complexes that prevent syntaxin from binding to the other neuronal SNAREs[31]. Likewise, the yeast Sec1p homolog Sly1p appears to play a similar role in endoplasmic reticulum to Golgi transport, binding tightly to the Sso1p homolog Sed5p[28,39]. In this case, the Rab protein Ypt1p facilitates dissociation of Sly1p, allowing Sed5p to bind v-SNAREs[30]. By analogy, Sec1p and Sec4p may act in concert, perhaps with the assistance of other proteins, to catalyze Sso1p–Sec9p assembly. Thereafter, ternary complex formation would be rapid and spontaneous.

Several potentially related functions have been ascribed to N-terminal regions of syntaxin analogous to Sso1NT. Syntaxin residues 1–193 inhibit the weak binary interaction between a C-terminal region (residues 194–267) and the v-SNARE VAMP/synaptobrevin[21]. It has also been reported that N-terminal regions of syntaxin are required for the disassembly of SNARE complexes by NSF/SNAPs[40,41]. The apparent difference in stoichiometry between yeast (1:1) and neuronal (2:1) binary complexes[15,25,26] suggests that the neuronal SNARE assembly pathway may differ in some respects from the yeast pathway. Nonetheless, it is attractive to speculate based on our results that an N-terminal domain of syntaxin may function to inhibit reassembly in NSF/SNAP disassembly reactions, rather than by being required for disassembly directly. Kinetic analysis of syntaxin–SNAP-25 assembly will be necessary to test this possibility.

Structural implications

Results presented here are consistent with the hypothesis, based on sequence analysis and site-directed mutagenesis[23,24,42], that SNARE proteins form α-helical coiled coils upon complex formation. The SNARE domains involved in complex formation are individually unfolded, as expected for polypeptide segments that, upon combination, form coiled coils. Furthermore, binary and ternary SNARE complexes display unusually high α-helix contents (70% and >85% respectively); for Sso1CTa–Sec9CT–Snc2p, this implies that fewer than seventy (of 451) residues occupy non-helical conformations. Binary, and particularly ternary, SNARE complexes are thermostable, as has been found for other long coiled coils (for example, the triple-stranded coiled coil cores of influenza and HIV fusion proteins[43,44]). For Sso1p, the C-terminal region predicted to form a coiled coil contributes most of this stability.

The dimensions of the rod-like core of the homologous neuronal SNARE complex (approximately 4 × 13 nm) are also consistent with a coiled coil[7]. Tagging experiments show that both syntaxin and VAMP run the entire length of the neuronal SNARE complex, with the N-terminal ends of both proteins at one end of the rod and both C-terminal ends at the other[7,8]. Therefore, it seems likely that each SNARE contributes at least one helix to a multi-stranded coiled coil. One attractive model, based on sequence analysis, is that Sso1p and Snc2p each contribute one helix to a four-stranded coiled coil, while Sec9CT contributes two[23]. This model draws support from recent biochemical analyses of neuronal SNARE complexes in which two discrete segments of the Sec9 homolog SNAP-25 are protected from trypsin digestion in ternary SNARE complexes[45,46], but definitive confirmation awaits high-resolution structural analysis.

Methods

Plasmid assembly. Genes encoding yeast post-Golgi SNAREs were obtained from Sirkka Keränen (Sso1p, Sso2p), Jeffrey Gerst (Snc2p), and Patrick Brennwald (Sec9p). PCR amplification was used to introduce restriction sites used for cloning coding sequences into expression plasmids (PCR primer sequences are available upon request). Plasmids expressing Factor X_a (FX_a)-cleavable GST fusion proteins were assembled by cloning Sso1p[1–265] (Sso1p), Sso1p[192–265] (Sso1CT), Sso1p[146–265] (Sso1CTa), Sso2p[1–269] (Sso2p), Sso2p[196–269] (Sso2CT), and Snc2p[1–92] (Snc2p) into pGEX-3X (Pharmacia Biotech). After FX_a cleavage, one or more heterologous residues remain at the N-terminus of Snc2p (Gly-), Sso1CT (Gly-Ile-Arg-), and Sso1CTa (Gly-Ile-). Sso1p, Sso1p[1–145] (Sso1NT), Sso2p, and Sec9p[416–651] (Sec9CT) were cloned into the T7 expression plasmid pLM-1[47]. All coding regions were sequenced to confirm that no errors were introduced by PCR.

We noted a discrepancy between the amino acid sequence of Sso2p derived from YEpSSO2[12] and the sequence deposited in the Yeast Protein Database, resulting in the amino acid change $Glu_{222} \rightarrow Lys$. Therefore, we modified our pGEX-Sso2p, pGEX-Sso2CT, and pLM1-Sso2p expression plasmids by PCR to match the amino acid sequence in the Yeast Protein Database, and used the corresponding proteins throughout these studies.

Purification of recombinant proteins. GST fusion proteins were purified from *E. coli* BL21 cells carrying pGEX expression plasmids essentially as described[48]. Soluble Sso1CT, Sso1CTa, and Snc2p were released by FX_a cleavage of GST fusions immobilized on glutathione agarose (Sigma). FX_a purified from bovine blood[49] was added to the slurry at an enzyme:substrate ratio of ~1:200 (w:w) and the mixture incubated at 4 °C for 2 h, after which the protease was inactivated by adding 1,5-DNS-GGACK,HCl (CalBiochem) to 2 μM. The Sso1CT or SsoCTa released by FX_a was further purified by anion exchange, while Snc2p was further purified by cation exchange (MonoQ or MonoS, respectively; Pharmacia). Pure fractions were concentrated by ultrafiltration (Millipore Ultrafree-15) and stored frozen at -80 °C.

Sso1p, Sso1NT, Sso2p and Sec9CT were purified from BL21(DE3) cells carrying pLM1-derived expression plasmids. Overproduction of Sec9CT was limited by poor codon usage: in the Sec9CT mRNA, 17 of 21 Arg codons require the ArgU tRNA, present in *E. coli* in limiting quantities[50]. Therefore, to obtain reasonable expression of Sec9CT, it was necessary to cotransform cells with a multicopy plasmid (pDC952) carrying the ArgU tRNA gene, a kind gift from James Walker (University of Texas, Austin). Sso1p and Sso2p were purified using DEAE Sepharose, Q Sepharose, Phenyl Sepharose, Superdex 75, and MonoQ columns (Pharmacia). Sec9CT was purified using Q Sepharose, Phenyl Sepharose, Superdex 200, and MonoQ columns. Sso1NT was purified using Q Sepharose and Superdex 75 columns. Complete experimental details are available from the authors upon request. Purified proteins were concentrated using a stirred cell with YM10 ultrafiltration membranes (Amicon) and stored frozen at -80 °C.

Purified Sso1p, Sso1CT, Sso1CTa, Sso1NT, Sec9CT and Snc2p were at least 90% homogeneous as judged by overloaded Coomassie-stained SDS-PAGE gels. The precise mass (±0.01%) of each protein was confirmed by electrospray ionization mass spectrometry. Protein concentrations were determined by absorbance in 6 M guanidine hydrochloride[51] or by a quantitative ninhydrin assay[52] using leucine as a standard. Where both methods could be used, results agreed within 10%.

Solid-phase binding assays. Glutathione Sepharose beads with immobilized GST-Sso1p, -Sso1CT, -Sso2p, or -Sso2CT were equilibrated in binding buffer (10 mM potassium phosphate, 140 mM KCl, pH 7.4). Soluble proteins were dialyzed against the same buffer. Approximately equimolar mixtures of glutathione-immobilized and soluble protein(s) (7 μM each) were incubated in binding buffer 12–14 h at 4 °C with mixing. The resin was pelleted and the supernatants were removed; pellets were washed four times with binding buffer. Equivalent aliquots of supernatants and pellets were analyzed on SDS-PAGE gels stained with Coomassie Blue R-250.

Circular dichroism spectroscopy. Samples for circular dichroism (CD) spectra and temperature melts were prepared by adding the appropriate proteins to a final concentration of 5 μM each in binding buffer, and then preincubating the sample at 18 °C to allow complex formation to proceed to completion. For complexes involving Sso1p, where complex formation is not complete after 24 h, complexes were prior to CD analysis. For kinetic analysis of SNARE complex assembly, samples were mixed manually and immediately transferred into the spectrometer; the resulting dead time (15–45 s) was factored into the data analysis (see below). Binary Sso1p–Sec9CT complexes were isolated by mixing equimolar amounts of Sso1p and Sec9CT, incubating 18 h at 18 °C in binding buffer, purifying the complex on a MonoQ column at pH 7, and exchanging the complex back into binding buffer.

CD data were collected using an AVIV 62DS CD spectrometer. Spectra from three consecutive scans (250–200 nm, 1 s averaging time, 0.5 nm steps) were averaged. For thermal unfolding experiments, data at 222 nm were recorded (1 min temperature equilibration, 0.5 min averaging time, 1 °C steps). Complex formation was monitored by recording data at 222 nm at 5 s intervals after manual mixing. Spectra and melts were acquired using a 1 mm pathlength quartz cuvette; kinetic measurements were acquired using either 1 cm or 1 mm pathlength quartz cuvettes. α-helix content was estimated from $[\theta]_{222}$[53].

Analytical ultracentrifugation. Sedimentation equilibrium experiments were performed using a Beckman Optima XL-A analytical ultracentrifuge with an An60 Ti rotor. Snc2p, Sec9CT, Sso1p and Sso1CT were centrifuged individually and as equimolar binary and ternary mixtures. For complexes, several concentrations between 1 and 10 μM and multiple speeds from 4,000–20,000 r.p.m. were used at either 4 °C (binary complex) or 18 °C (ternary complex). Absorbance was measured at several wavelengths between 235 and 288 nm depending on the absorbance spectra of individual samples. Data were analyzed using the HID software from the Analytical Ultracentrifugation Facility at the University of Connecticut and a buffer density of 1.0032 g ml^{-1}.

Gel filtration analysis of SNARE assembly. Mixtures containing equimolar Sso1p and Sec9CT in binding buffer were incubated at 18 °C. At various times during this incubation, samples were removed, centrifuged at 14,000g for 10 min, and injected onto a Superdex 200

10/30 column (4 °C) pre-equilibrated in binding buffer. Peaks monitored by absorbance at 280 nm were integrated using the program FPLC Director (Pharmacia). For the kinetic analysis shown in Fig. 6a, equal amounts of protein (200 µl for 5 µM samples; 20 µl for 50 µM samples) were injected onto the column. For Sso1NT–Sso1CT binding experiments, 250 µl samples (not centrifuged) were injected onto the Superdex 200 10/30 column running at 0.7 ml min^{-1}.

Kinetic analysis. The rate constant, k, for the formation of each SNARE complex was calculated by fitting kinetic data to the equation $\theta(t) = \theta_0 + (\theta_\infty - \theta_0)(A_0kt)/(A_0kt + 1)$ using the program Kaleidagraph (Abelbeck Software). This equation was derived from the integrated rate law of the second order reaction $A + B \rightarrow P$ for the case in which $A_0 = B_0$. In this treatment, $\theta(t)$ is the value of the experimental observable (peak area for gel filtration experiments or mean residue ellipticity for CD experiments) at time t, θ_0 is the experimental observable at t = 0, θ_∞ is the experimental observable at t = ∞, A_0 (= B_0) is the initial concentration of each reactant in molar units (M), k is the rate constant in M^{-1} s^{-1}, and t is the time since mixing in s. For the CD kinetic experiments, θ_0 was calculated as the mean residue ellipticity value of a non-interacting mixture of the appropriate SNAREs. For gel filtration experiments, θ_0 was fitted together with the rate constant, k.

Acknowledgments

We thank P. Brennwald, J. Gerst, S. Keränen and J. Walker for plasmids, S. Kyin and D. Little for DNA sequencing and mass spectrometry, and G. Waters, P. Brennwald, J. Carey, P. Hanson, G. McLendon, and A. Nagi for discussion and critical comments on the manuscript. The analytical ultracentrifuge was purchased with funds from a grant to R.F. from the Zimmer Corporation. This work was funded in part by an American Heart Association Fellowship (M.M.) and Searle Scholar and Beckman Young Investigator awards (F.M.H.).

Received 17 June, 1998; accepted 29 July, 1998.

1. Söllner, T. *et al.* SNAP receptors implicated in vesicle targeting and fusion. *Nature* **362**, 318-324 (1993).
2. Pfeffer, S.R. Transport vesicle docking: SNAREs and associates. *A. Rev. Cell Dev. Biol.* **12**, 441-461 (1996).
3. Söllner, T., Bennett, M.K., Whiteheart, S.W., Scheller, R.H. & Rothman, J.E. A protein assembly-dissassembly pathway in vitro that may correspond to sequential steps of synaptic vesicle docking, activation, and fusion. *Cell* **75**, 409-418 (1993).
4. Nichols, B.J., Ungermann, C., Pelham, H.R.B., Wickner, W.T. & Haas, A. Homotypic vacuolar fusion mediated by t- and v-SNAREs. *Nature* **387**, 199-202 (1997).
5. Rothman, J.E. & Warren, G. Implications of the SNARE hypothesis for intracellular membrane topology and dynamics. *Curr. Biol.* **4**, 220-233 (1994).
6. Weber, T. *et al.* SNAREpins: minimal machinery for membrane fusion. *Cell* **92**, 759-772 (1998).
7. Hanson, P.I., Roth, R., Morisaki, H., Jahn, R. & Heuser, J.E. Structure and conformational changes in NSF and its membrane receptor complexes visualized by quick-freeze/deep-etch electron microscopy. *Cell* **90**, 523-535 (1997).
8. Lin, R.C. & Scheller, R.H. Structural organization of the synaptic exocytosis core complex. *Neuron* **19**, 1087-1094 (1997).
9. Hughson, F.M. Enveloped viruses: a common mode of membrane fusion? *Curr. Biol.* **7**, R565-R569 (1997).
10. Protopopov, V., Govindan, B., Novick, P. & Gerst, J.E. Homologs of the synaptobrevin/VAMP family of synaptic vesicle proteins function on the late secretory pathway in S. cerevisiae. *Cell* **74**, 855-861 (1993).
11. Brennwald, P. *et al.* Sec9 is a SNAP-25-like component of a yeast SNARE complex that may be the effector of Sec4 function in exocytosis. *Cell* **79**, 245-258 (1994).
12. Aalto, M.K., Ronne, H. & Keränen, S. Yeast syntaxins Sso1p and Sso2p belong to a family of related membrane proteins that function in vesicular transport. *EMBO J.* **12**, 4095-4104 (1993).
13. Ferro-Novick, S. & Jahn, R. Vesicle fusion from yeast to man. *Nature* **370**, 191-193 (1994).
14. Hanson, P.I., Heuser, J.E. & Jahn, R. Neurotransmitter release — four years of SNARE complexes. *Curr. Opin. Neurobiol.* **7**, 310-315 (1997).
15. Rossi, G., Salminen, A., Rice, L.M., Brünger, A.T. & Brennwald, P. Analysis of a yeast SNARE complex reveals remarkable similarity to the neuronal SNARE complex and a novel function for the C terminus of the SNAP-25 homolog, Sec9. *J. Biol. Chem.* **272**, 16610-16617 (1997).
16. Veit, M., Söllner, T.H. & Rothman, J.E. Multiple palmitoylation of synaptotagmin and the t-SNARE SNAP-25. *FEBS Lett.* **385**, 119-123 (1996).
17. Couve, A. & Gerst, J.E. Yeast Snc proteins complex with Sec9: functional interactions between putative SNARE proteins. *J. Biol. Chem.* **269**, 23391-23394 (1994).
18. Hayashi, T. *et al.* Synaptic vesicle membrane fusion complex: action of clostridial neurotoxins on assembly. *EMBO J.* **13**, 5051-5061 (1994).
19. Lupas, A., Van Dyke, M. & Stock, J. Predicting coiled coils from protein sequences. *Science* **252**, 1162-1164 (1991).
20. Berger, B. *et al.* Predicting coiled coils by use of pairwise residue correlations. *Proc. Natl Acad. Sci. USA* **92**, 8259-8263 (1995).
21. Calakos, N., Bennett, M.K., Peterson, K.E. & Scheller, R.H. Protein-protein interactions contributing to the specificity of intracellular vesicular trafficking. *Science* **263**, 1146-1149 (1994).
22. Chapman, E.R., An, S., Barton, N. & Jahn, R. SNAP-25, a t-SNARE which binds to both syntaxin and synaptobrevin via domains that may form coiled coils. *J. Biol. Chem.* **269**, 27427-27432 (1994).
23. Weimbs, T. *et al.* A conserved domain is present in different families of vesicular fusion proteins: a new superfamily. *Proc. Natl. Acad. Sci. USA* **94**, 3046-3051 (1997).
24. Fasshauer, D., Bruns, D., Shen, B., Jahn, R. & Brünger, A.T. A structural change occurs upon binding of syntaxin to SNAP-25. *J. Biol. Chem.* **272**, 4582-4590 (1997).
25. Fasshauer, D., Otto, H., Eliason, W.K., Jahn, R. & Brünger, A.T. Structural changes are associated with soluble N-ethylmaleimide-sensitive fusion protein attachment protein receptor complex formation. *J. Biol. Chem.* **272**, 28036-28041 (1997).
26. Rice, L.M., Brennwald, P. & Brünger, A.T. Formation of a yeast SNARE complex is accompanied by significant structural changes. *FEBS Lett.* **415**, 49-55 (1997).
27. Rothman, J.E. & Söllner, T.H. Throttles and dampers: controlling the engine of membrane fusion. *Science* **276**, 1212-1213 (1997).
28. Søgaard, M. *et al.* A rab protein is required for the assembly of SNARE complexes in the docking of transport vesicles. *Cell* **78**, 937-948 (1994).
29. Lian, J.P., Stone, S., Jiang, Y., Lyons, P. & Ferro-Novick, S. Ypt1p implicated in v-SNARE activation. *Nature* **372**, 698-701 (1994).
30. Lupashin, V.V. & Waters, M.G. t-SNARE activation through transient interaction with a Rab-like guanosine triphosphatase. *Science* **276**, 1255-1258 (1997).
31. Pevsner, J. *et al.* Specificity and regulation of a synaptic vesicle docking complex. *Neuron* **13**, 353-361 (1994).
32. Garcia, E.P., Gatti, E., Butler, M., Burton, J. & De Camilli, P. A rat brain Sec1 homologue related to Rop and UNC18 interacts with syntaxin. *Proc. Natl. Acad. Sci. USA* **91**, 2003-2007 (1994).
33. Cornille, F., Goudreau, N., Ficheux, D., Niemann, H. & Roques, B.P. Solid-phase synthesis, conformational analysis and in vitro cleavage of synthetic human synaptobrevin II 1-93 by tetanus toxin L chain. *Eur. J. Biochem.* **222**, 173-181 (1994).
34. Zitzewitz, J.A., Bilsel, O., Luo, J., Jones, B.E. & Matthews, C.R. Probing the folding mechanism of a leucine zipper peptide by stopped-flow circular dichroism spectroscopy. *Biochemistry* **34**, 12812-12819 (1995).
35. Govindan, B. & Novick, P. Development of cell polarity in budding yeast. *J. Exp. Zool.* **273**, 401-424 (1995).
36. Terbush, D.R., Maurice, T., Roth, D. & Novick, P. The Exocyst is a multiprotein complex required for exocytosis in Saccharomyces cerevisiae. *EMBO J.* **15**, 6483-6494 (1996).
37. Finger, F.P., Hughes, T.E. & Novick, P. Sec3p is a spatial landmark for polarized secretion in budding yeast. *Cell* **92**, 559-571 (1998).
38. Mayer, A. & Wickner, W. Docking of yeast vacuoles is catalyzed by the ras-like GTPase Ypt7p after symmetric priming by Sec18p (NSF). *J. Cell Biol.* **136**, 307-317 (1997).
39. Grabowski, R. & Gallwitz, D. High-affinity binding of the yeast cis-Golgi t-SNARE, Sed5p, to wild-type and mutant Sly1p, a modulator of transport vesicle docking. *FEBS Lett.* **411**, 169-172 (1997).
40. Hanson, P.I., Otto, H., Barton, N. & Jahn, R. The N-ethylmaleimide-sensitive fusion protein and α-SNAP induce a conformational change in syntaxin. *J. Biol. Chem.* **270**, 16955-16961 (1995).
41. Hayashi, T., Yamasaki, S., Nauenburg, S., Binz, T. & Niemann, H. Disassembly of the reconstituted synaptic vesicle membrane fusion complex *in vitro*. *EMBO J.* **14**, 2317-2325 (1995).
42. Kee, Y., Lin, R.C., Hsu, S.-C. & Scheller, R.H. Distinct domains of syntaxin are required for synaptic vesicle fusion complex formation and dissociation. *Neuron* **14**, 991-998 (1995).
43. Bullough, P.A., Hughson, F.M., Skehel, J.J. & Wiley, D.C. Structure of influenza haemagglutinin at the pH of membrane fusion. *Nature* **371**, 37-43 (1994).
44. Lu, M., Blacklow, S.C. & Kim, P.S. A trimeric structural domain of the HIV-1 transmembrane glycoprotein. *Nature Struct. Biol.* **2**, 1075-1082 (1995).
45. Poirer, M.A. *et al.* Protease resistance of syntaxin:SNAP-25:VAMP complexes: implications for assembly and structure. *J. Biol. Chem.* **273**, 11370-11377 (1998).
46. Fasshauer, D., Eliason, W.K., Brünger, A.T. & Jahn, R. Identification of a minimal core of the synaptic SNARE complex sufficient for reversible assembly and disassembly. *Biochemistry* **37**, 10354–10362 (1998).
47. MacFerrin, K.D., Chen, L., Terranova, M.P., Schreiber, S.L. & Verdine, G.L. Overproduction of proteins using expression-cassette polymerase chain reaction. *Meth. Enz.* **217**, 79-102 (1993).
48. Smith, D.B. & Johnson, K.S. Single-step purification of polypeptides expressed in Escherichia coli as fusions with glutathione S-transferase. *Gene* **67**, 31-40 (1988).
49. Nagai, K. & Thøgersen, H.C. Synthesis and sequence-specific proteolysis of hybrid proteins produced in *Escherichia coli*. *Meth. Enz.* **153**, 461-481 (1987).
50. Spanjaard, R.A., Chen, K., Walter, J.R. & van Duin, J. Frameshift suppression at tandem AGA and AGG codons by cloned tRNA genes: assigning a codon to argU tRNA and T4 $tRNA^{Arg}$. *Nucleic Acids Res.* **18**, 5031-5036 (1990).
51. Edelhoch, H. Spectroscopic determination of tryptophan and tyrosine in proteins. *Biochemistry* **6**, 1948-1954 (1967).
52. Rosen, H. A modified ninhydrin colorimetric analysis for amino acids. *Arch. Biochem. Biophys.* **67**, 10-15 (1957).
53. Scholtz, J.M., Qian, H., York, E.J., Stewart, J.M. & Baldwin, R.L. Parameters of helix-coil transition theory for alanine-based peptides of varying chain lengths in water. *Biopolymers* **31**, 1463-1470 (1991).